

Analytical Methods

Accepted Manuscript



This is an *Accepted Manuscript*, which has been through the Royal Society of Chemistry peer review process and has been accepted for publication.

Accepted Manuscripts are published online shortly after acceptance, before technical editing, formatting and proof reading. Using this free service, authors can make their results available to the community, in citable form, before we publish the edited article. We will replace this *Accepted Manuscript* with the edited and formatted *Advance Article* as soon as it is available.

You can find more information about *Accepted Manuscripts* in the [Information for Authors](#).

Please note that technical editing may introduce minor changes to the text and/or graphics, which may alter content. The journal's standard [Terms & Conditions](#) and the [Ethical guidelines](#) still apply. In no event shall the Royal Society of Chemistry be held responsible for any errors or omissions in this *Accepted Manuscript* or any consequences arising from the use of any information it contains.

ARTICLE

A versatile and robust electrochemical flow cell with a boron-doped diamond electrode for simultaneous determination of Zn²⁺ and Pb²⁺ ions in water samples

Vagner Bezerra dos Santos^{a,*}, Elson Luiz Fava^a, Osmundo Dantas Pessoa-Neto^a, Silmara Rossana Bianchi^b, Ronaldo Censi Faria^a and Orlando Fatibello-Filho^a

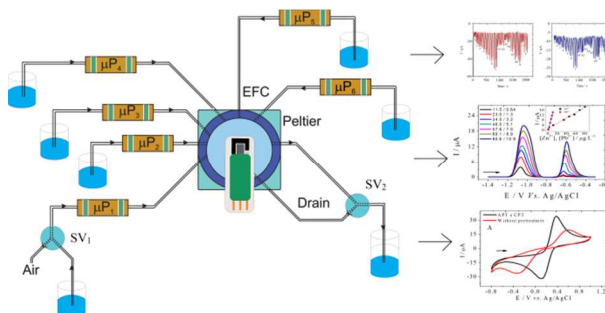
Cite this: DOI: 10.1039/x0xx00000x

Received 00th January 2012,
Accepted 00th January 2012

DOI: 10.1039/x0xx00000x

www.rsc.org/

Graphical Abstract



Automation of multiple pulse amperometry, anodic stripping and cyclic voltammetry using a thermostated electrochemical flow cell with distinct flow systems.

COMMUNICATION

Cite this: DOI: 10.1039/x0xx00000x

Received 00th January 2012,

Accepted 00th January 2012

DOI: 10.1039/x0xx00000x

www.rsc.org/

A versatile and robust electrochemical flow cell with a boron-doped diamond electrode for simultaneous determination of Zn²⁺ and Pb²⁺ ions in water samples

Vagner Bezerra dos Santos^{a,*}, Elson Luiz Fava^a, Osmundo Dantas Pessoa-Neto^a, Silmara Rossana Bianchi^b, Ronaldo Censi Faria^a and Orlando Fatibello-Filho^a

A versatile and robust thermostated electrochemical flow cell (EFC) with a boron-doped diamond electrode (BDD) detector was employed to perform two distinct flow-injection electrochemical approaches. In the first, a differential pulse anodic stripping voltammetry (DPASV) using a flow-batch analysis (FBA) is proposed. In the second, a multiple pulse amperometry (MPA) employing multicommutation flow analysis (MCFA) is also presented. Both approaches were employed to simultaneously determine Zn²⁺ and Pb²⁺ in water samples. For this, a screen-printed electrode (SPE) was developed, and a BDD electrode was coupled to it and was inserted into the EFC. Employing the FBA with the DPASV technique, two analytical curves in concentration ranges from 11.5 to 80.6 µg L⁻¹ and 0.64 to 10.9 µg L⁻¹ for simultaneous determination of Zn²⁺ and Pb²⁺, respectively, were obtained. Moreover, limits of detection (LD) of 0.62 µg L⁻¹ and 0.19 µg L⁻¹ were estimated respectively and a sampling frequency of 12 h⁻¹ was obtained. For MCFA with MPA, analytical curves from 830 to 4980 µg L⁻¹ and 140 to 820 µg L⁻¹ for simultaneous determination of Zn²⁺ and Pb²⁺ with LDs of 220.0 µg L⁻¹ and 41.0 µg L⁻¹ and a sampling frequency of 67 h⁻¹ were obtained. The developed EFC allowed a full on-line automation of the methods, covering the pretreatment of BDD, addition of standards solutions, dilutions, thermostated control, and detection with and without electrochemical preconcentration. In addition, the low waste generation of only 700 µL may be useful for green chemistry purposes and sustainable research.

Introduction

Boron-doped diamond (BDD) has been widely used for electroanalytical chemistry purposes, especially in the last two decades.^{1,2} Diamond is naturally insulated; however, when doped with boron atoms, it presents good electrical conductivity, which is required for electrochemical applications. The doping processes can reach the order of 1.0×10^{20} atoms of boron per cm³, which corresponds to one boron atom per 1000 carbon atoms.^{2,3} Typical doping levels between 1000 and 10,000 ppm of boron are used. Characteristics such as good electrical conductivity, low adsorption, high chemical inertness, low residual current, insensitivity to dissolved oxygen, and a large work potential window, with high overpotentials for H_{2(g)} and O_{2(g)}, are the main characteristics of the BDD electrode for analytical applications.³

BDD electrodes should undergo some pretreatment or functionalization prior to use, which modifies the surface with hydrogen-terminated or oxygen-terminated, or even functional, groups on its surface.⁴ Simple techniques such as chronopotentiometry can be used to perform the pretreatments by applying negative current (cathodic pretreatment, CPT) and/or positive current (anodic pretreatment, APT).^{5,6}

These electrodes have been employed in a large number of applications, such as electrochemical degradation of pollutant

compounds,⁷⁻¹⁰ or used in the manufacture of biosensors and/or immunosensors,³ as well as being modified with nanoparticles¹ and to prepare screen-printed¹¹. The BDD electrodes have been used mostly in batch procedures using conventional electrochemical cells.^{1,6}

Focusing on the determination of metal ions, the batch approaches are usually associated with preconcentration techniques, such as anodic stripping voltammetry (ASV) and adsorptive anodic stripping voltammetry (AdASV).² In this context, electroactive cations, such as Cd²⁺, Pb²⁺, Cu²⁺, Zn²⁺, Ag⁺, Pd²⁺, and Hg²⁺, have been determined by employing BDD in various samples, resulting in detection limits as low as µg L⁻¹ or ng L⁻¹, using differential pulse anodic stripping voltammetry (DPASV) or square-wave anodic stripping voltammetry (SWASV).^{2,12-17} A very interesting application of BDD electrodes using these techniques involves the possibility of simultaneous determinations.^{2,14} However, in batch analysis, the sampling frequency is not favorable, due to the preconcentration steps, which make its use difficult in routine analysis or for a larger number of samples.

To overcome this drawback, amperometry coupled to flow analyses are particularly useful,^{5,18-21} especially when pulsed amperometric detection (PAD)²¹ or multiple pulse amperometry (MPA)^{22,23} are employed. In fact, amperometry with flow

analyses has presented a greater level of automation, and consequently, a higher sampling frequency and lower consumption of reagents with a lower waste generation than batch procedures.²¹ In both techniques, pulses of potential are sequentially applied with times as short as 100 ms, but in the PAD only one current signal is measured, while for the MPA, for each applied potential, an independent current is measured.²³ PAD or MPA applied using a BDD usually provide good repeatability, mainly due to reduced adsorption on the electrode surface along the analysis, which is a known limitation of solid electrodes.^{21,23}

These electrodes combined with PAD or MPA have been applied for determination of drugs,²⁴ phenolic antioxidant compounds in food,²⁵ and in the development of biosensors and immunosensors.³ In general, the use of these techniques together with FIA (flow injection analysis), SIA (sequential injection analysis), or BIA (batch injection analysis)²² has provided a sampling frequency between 50 and 130 h⁻¹, with a repeatability of less than 5.0%. Moreover, volumes of sampling and waste less than 1000 μL are commonly used, depending on the configuration of the EFC employed.

In this context, we introduce herein two distinct flow electrochemical methods based on DPASV with flow-batch analysis (FBA), and the MPA with multicommutation flow analysis (MCFA) for simultaneous determination of Zn²⁺ and Pb²⁺ in water samples. For use in both methods, a thermostated EFC was developed to carry out thermostatic control, pretreatment of the BDD, construction of analytical curves, dilutions, and standard addition procedures with a fully on-line automated flow system. The thermostated temperature control is essential, mainly for *in loco* electrochemical measurements, especially for environmental analyses.²⁶

Experimental

Apparatus and instrumentation

The electroanalytical measurements were carried out using a potentiostat/galvanostat Autolab PGSTAT128N (Metrohm Autolab, Switzerland) controlled by GPES or Nova software (Metrohm Autolab, Switzerland). An inductively coupled plasma optical emission spectrometer (ICP-OES) model AX-CCD (Varian, Australia) was used to reference method. A lab-made actuator driven by a 6008 USB interface (NI, USA) was controlled using software programmed in Labview (NI, USA). The solenoid micropumps (μPs) model 120SP1250-4EE and 120SP1220-4EE (Coleparmer, USA) that pump 50 μL and 20 μL per pulse, the three-way solenoid valves (Neptune Research, USA) model 161TO31, and 0.8 mm i.d. polypropylene tubes were used in the flow systems. A microcontrolled board with an 18F4550 microcontroller (Microchip, USA) embedded was developed to drive a Peltier thermoelectric cell (Danvic, Brazil) model HTC-40-03-15.4, and a LM35 temperature sensor (Texas Instruments, USA), using a 12 V battery 7 Ah⁻¹ (Unipower, Brazil). A heat press PTM 30 (F1 suprimentos, Brazil) was used to manufacture the screen-printed electrodes (SPE). Diamond electrodes doped with 8,000 ppm boron, used as the working electrode (WE), were purchased from the *Centre Suisse Electronique et de microtechnique SA* in Neuchâtel (Switzerland). The pseudo-reference electrode (pseudo-RE) and counter electrode (CE) were manufactured by applying a conductive silver epoxy resin and a conductive graphite ink (Electron Microscopy Sciences, USA), respectively. Printed circuit boards (PCB) were used for confection of the SPEs.

Chemicals and samples

Phosphate (0.2 mol L⁻¹, pH 4.0 and pH 5.0), acetic acid/acetate (0.2 mol L⁻¹, pH 4.0 and pH 4.5), and Britton-Robinson (BR) (0.04 mol L⁻¹, pH 2.0, 4.0 and 6.0) buffer solutions were prepared. H₂SO₄ solutions at 1.0, 0.5, and 0.1 mol L⁻¹ were also prepared.

Solutions of certified metal ions from the National Institute of Standards and Technology (USA), 1000 mg L⁻¹ of Zn²⁺ and Pb²⁺ dissolved in 0.1 mol L⁻¹ HNO₃, were purchased from Merck (Germany). Dilutions of these solutions were performed employing the acetic acid/acetate (0.2 mol L⁻¹, pH 4.0) solution. Certified river water (1643e Trace Elements in Water, NIST) with concentrations of Zn²⁺ and Pb²⁺ of 78.5 \pm 2.2 $\mu\text{g L}^{-1}$ and 19.63 \pm 0.21 $\mu\text{g L}^{-1}$, respectively, were employed for accuracy tests. Deionized water (resistivity > 1.8 M Ω cm) acquired from a Milli-Q system (Millipore, USA) was used. All reagents used were of analytical grade acquired from the Acros (USA), Sigma (USA), and Merck (Germany).

The water samples analyzed were: wastewater and tap water from the Department of Chemistry from the Federal University of São Carlos (Brazil), and samples collected from three distinct points of the Monjolinho Lake in São Carlos (Brazil). Moreover, water samples obtained from the pretreatment of water substations (SANEPAR, Brazil), wastewater from the petrochemical industry (Petrobras, Brazil), and from the seawater samples (Alicante, Spain) were studied. The samples were previously collected, packed in styrofoam, and kept between 0°C and 5°C. Samples were filtered employing 0.45- μm filter paper (Whatman, USA) and a vacuum pump.

All the electrochemical data presented were acquired at a temperature of 25 \pm 1°C, which was controlled using the thermostated electrochemical flow cell developed for this purpose.

BDD coupled to the SPE

In Fig. 1 (A), a typical BDD electrode used for batch procedure is presented. For this, the BDD was immobilized over a copper substrate (1) using a small amount of solder (2), and posteriorly, epoxy resin was applied for electrical insulation (3).

In Fig. 1 (B), the SPE with the BDD coupled to it is shown (SPE-BDD). For this, a design was created in CorelDraw X3, printed on transfer paper with toner from a laser printer, and it was transferred to the PCB by heating at 200°C for 60 s. Next, the copper layer was removed by using a saturated solution of iron (III) chloride. Subsequently, the conductive graphite ink and silver epoxy were manually applied. To fix the BDD onto the SPE, a small amount of solder was used (1). After the fixation of the BDD, the heating was rapidly finished to avoid damage of the electrode (2). Epoxy resin was manually applied to electrically isolate the SPE-BDD (3). The fixation of the BDD with solder was possible due to a thin layer of gold at the base of the commercially available BDD. The dimensions of the electrodes were the following: WE: 25.7 mm², CE: 77.70 mm², pseudo-RE: 6.0 mm², width: 12.0 mm, length: 40.0 mm. The conventional BDD electrode has 3.0 \times 8.5 cm (width \times length) dimensions.

The SPE-BDD produced has reduced dimensions that needed to be coupled to a miniaturized EFC. More details to produce the SPE can be seen in a previous work.²⁶

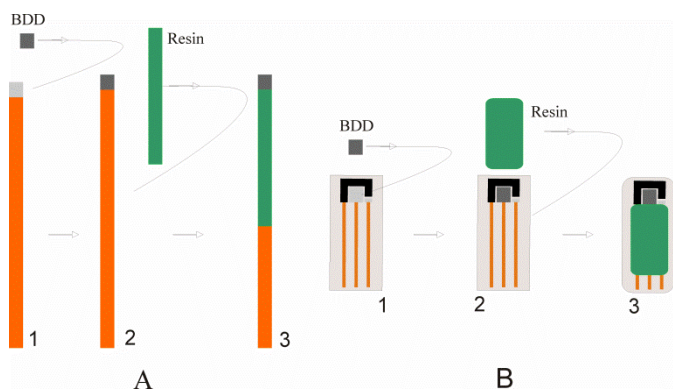


Fig. 1. Steps to produce the conventional electrode of the BDD coupled to a copper rod (A) and to produce the BDD embedded in the SPE (B).

SPE-BDD coupled to the EFC

Two flow electrochemical methods, FBA with DPASV (FBA-DPASV) and MCFA with MPA (MCFA-MPA), were applied to the SPE-BDD coupled to the thermostated EFC, Fig. 2.

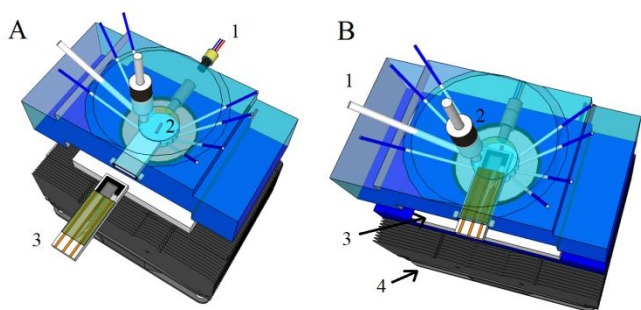


Fig. 2. View from above of the coupling of the SPE-BDD and the temperature sensor (A) into the EFC (B). The temperature sensor (1), a millimetric magnetic bar (2) used to stir the solution during the DPASV, and the SPE-BDD outside of the EFC (3) are shown (A). A Tygon tube was used as outlet flow (1) or, optionally, a stainless steel tube could be employed as an external CE. The external RE based on Ag/AgCl (3.0 mol L⁻¹ KCl) (2) could be used (B). Moreover, the Peltier cell (3) and an aluminum block with a coupled fan (4) are shown.

The EFC had an inner volume of 700 μL and was sealed by using two thermoplastic O-rings located in its circular base and around the SPE-BDD. The 0.8 mm i.d. blue tubing was used for inlet solutions into the EFC and the 3.0 mm i.d. Tygon white tubing for the outlet. The Peltier cell, the temperature sensor, and the fan employed for the thermostated control were driven by the microcontrolled board. A heatsick based on an aluminum block also was used. In upper side of the EFC, a stainless steel tube could be used to replace the Tygon tube for use as an optional external CE embedded in the SPE-BDD. Similarly, an external RE (Ag/AgCl, 3.0 mol L⁻¹ KCl) situated perpendicular to the upper face of the EFC can also be optionally used instead of the pseudo-RE from the SPE-BDD. More details of the EFC can be found in previous work.²⁶

The flow system control

An actuator board was developed and employed to control the solenoid micropumps (μP) and the three-way solenoid valves (SV) using a 6008 USB interface (NI, USA) were controlled by Labview (NI, USA) software. Thus, the μP s were employed to pump the solutions into the EFC. Using the actuator board for

each pulse of 0.5 s, aliquots of 20 μL or 50 μL were pumped according to the μP model used. Therefore, by controlling the time, flow rates of 40 $\mu\text{L s}^{-1}$, 100 $\mu\text{L s}^{-1}$, or multiples of them can be applied. The μP with capacity to pump 50 μL was used in MCFA-MPA in order to provide a high sampling frequency. On the other hand, for FBA-DPASV, in which a stopped-flow technique is necessary due to the preconcentration, the flow rate is not very significant, and the μP with 20 μL can be used.

Characterization of the flow systems

Fig. 3 presents the flow manifold for on-line pretreatment of the SPE-BDD and its application to determine Zn²⁺ and Pb²⁺ ions.

As can be seen in Fig. 3, when the SV₁ is OFF and the μP_1 and SV₂ are triggered, air is inserted into the EFC to dry and clean the EFC via the drain channel. The drain channel was used only in the FBA-DPASV. For the MCFA-MPA, the conventional outlet flow was employed by switching SV₁ and μP_1 ON with SV₂ OFF, which allowed a higher sampling frequency. The correct control of each μP allowed a series of analytical procedures, including on-line pretreatment of the BDD, construction of analytical curves, standard addition, recovery assays, and interference studies.

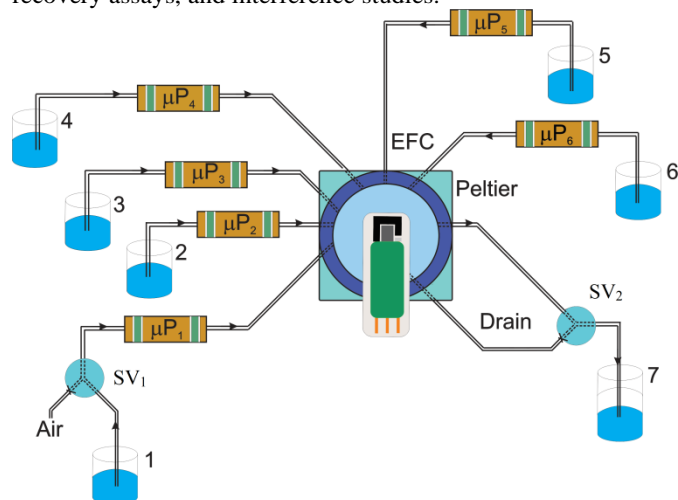


Fig. 3. Flow manifold developed for FBA-DPASV and MCFA-MPA. The μP_1 and μP_5 were used to pump 50 μL per pulse of acetic acid/acetate solution pH 4.0 (1) and 0.1 mol L⁻¹ H₂SO₄ (5), respectively. The μP_2 , μP_3 , μP_4 , and μP_6 pump 20 μL per pulse of the stock solutions of Zn²⁺ (2), Pb²⁺ (3), interferences (4), and samples (6), respectively. SV₁ and SV₂ are the three-way valves and the waste (7), respectively.

As shown in Fig. 3, the addition of solutions into the EFC was performed by multicommutation procedures, thus, the flow system can be classified as MCFA.²⁷ However, due to the flexibility of the EFC, the system can also be used in FBA²⁸ approach, and thus, a hybrid MCFA/FBA manifold is presented. However, we preferred to adopt the following classification: (1) flow procedures with detection by stopped-flow, *i.e.*, DPASV, are classified as FBA; and (2) those with detection in flow, *i.e.*, MPA, are described as MCFA-MPA.

The aforementioned classification is consistent because the procedures involving standard addition, mixing, dilution, drainage, and detection with stopped-flow performed inside of a chamber, *e.g.*, an EFC, are best characterized as FBA.²⁸ On the other hand, by performing the above procedures in flow, the characterization as MCFA²⁷ is more appropriate, because in the FBA system, usually transient signals are not obtained. This classification and settings were maintained for further

procedures. This flexibility of using different techniques was possible, mainly due to the appropriate inner volume of the EFC of 700 μL . Tests employing other models with inner volumes greater than 700 μL presents problems with the time residence of the sampling zone making wider the transient signal peak, reducing the sampling frequency, increasing the reagents consumption, and generating more waste.

Procedures for FBA and MCFA

For the FBA-DPASV, a series of steps is presented in Fig. S1 in Electronic Supplementary Information (ESI). At each step, n pulses of each μP and its switching ON time are presented, as well as for the solenoid valves (SV) and the stirrer (S) employed. Moreover, for further steps, the S was always switched ON, except for the steps 1 and 15.

First, the channels of the flow system were filled with respective solutions using the μP_2 , μP_3 , μP_4 , and μP_6 for 10 pulses, and μP_5 and μP_1 for 4 pulses. To apply the FBA approach the following procedures were performed: 700 μL of 0.1 mol L^{-1} H_2SO_4 solution were pumped towards the EFC through the activation of the μP_5 for 14 pulses to accomplish the pretreatment of BDD (step 2). The stopped-flow technique was carried out and the Peltier cell was activated for 30 s for the thermostatic control of the solutions at $25 \pm 1^\circ\text{C}$ (step 3). The effect of temperature variation was discussed in previous work and it is beyond the scope of this work.²⁶

Chronopotentiometric procedures were employed to perform the APT, applying current densities of 50 mA/cm^2 for 60 s, and -50 mA/cm^2 for 120 s for the CPT (step 4). Next, in step 5, drainage of the solution employing air was carried out by simultaneously switching μP_1 and SV_2 ON with a flow rate of 100 $\mu\text{L s}^{-1}$. Then, SV_1 was switched ON simultaneously with μP_1 for 30 pulses with SV_2 switched OFF to pump the supporting electrolyte solution to clean the EFC (step 6). In step 7, the drainage procedure was again performed. After this, the FBA system was employed to add the blank solution (supporting electrode) (step 8) or randomly any other step, *i.e.*, additions of the Zn^{2+} or Pb^{2+} solutions (steps 9 or 10), or aliquots of sample (step 12) by switching ON SV_1 , and the appropriate μP in pulses ranging from 1 to 35. For simultaneous determination of the Zn^{2+} and Pb^{2+} ions, the maximum pulses ranged from 1 to 17 for μP_1 , μP_2 , and μP_3 (step 11). Step 13 was similar to step 3 (thermostated control of the solutions), and, finally, the preconcentration and DPASV measurements (steps 14 and 15, respectively) were carried out. After this, a new analytical cycle was performed, by returning to step 5 (drainage of the solution into the EFC) to exchange the solutions or samples.

By applying the MCFA-MPA approach, the pretreatment of the BDD can be executed in flow, by continuously pumping of H_2SO_4 solution by switching ON the μP_5 . To reduce the consumption of the solution, a slow flow rate of 16 $\mu\text{L s}^{-1}$ was used. In the MCFA approach, the μP_1 and SV_1 were always switched ON to continuously pump buffer solution at a flow rate of 50 $\mu\text{L s}^{-1}$ toward the EFC to measure the background current. The aliquots of Zn^{2+} and/or Pb^{2+} ions solutions were injected into the EFC, and volumes were controlled by the number of pulses of μP_2 and μP_3 , respectively. The size of the sampling zone was proportional to the number of pulses and it was properly evaluated, such as the flow rate employed. By applying the MCFA-MPA, a significant reduction in the number of analytical steps was achieved, mainly by excluding the preconcentration and cleaning/drainage steps.

Pretreatment of the SPE-BDD surface

The BDD surface was pretreated by using chronopotentiometric procedures, employing a solution of 0.1 mol L^{-1} H_2SO_4 . To check the pretreatment, cyclic voltammetry using a 1.0×10^{-3} mol L^{-1} $\text{K}_3\text{Fe}(\text{CN})_6$ in 0.1 mol L^{-1} KCl solution was used. Moreover, comparative experiments employing the external CE and RE were also carried out.

Effect of the supporting electrolyte

The following supporting electrolytes were evaluated by cyclic voltammetry, taking into account the baseline current and potential window: phosphate buffer (0.2 mol L^{-1} , pH 4.0 and 5.0); solutions of 1.0, 0.5, and 0.1 mol L^{-1} H_2SO_4 ; acetic acid/acetate buffer (0.2 mol L^{-1} , pH 4.0 and 4.5); and Britton-Robinson (BR) buffer (0.04 mol L^{-1} , pH 2.0, 4.0 and 6.0).

Optimization of the DPASV and MPA parameters

The parameters for differential pulse anodic stripping voltammetry and multiple pulse amperometry were evaluated by evaluation of the electrochemical profile, resolution, and the magnitude of current. Moreover, the flow parameters from the MCFA system were also studied.

Interference study using the SPE-BDD

Interference studies on Zn^{2+} and Pb^{2+} determination were evaluated based on DPASV. For this, ions commonly encountered in natural water²⁹⁻³¹ were studied, including Li^+ , K^+ , Na^+ , Mg^{2+} , Ca^{2+} , Fe^{3+} , Cl^- , CO_3^{2-} , SO_4^{2-} , PO_4^{3-} , and NO_3^- . Moreover, Ni^{2+} , Cu^{2+} , Al^{3+} , Hg^{2+} , Cr^{3+} , Mn^{5+} , and humic acid (HA) from vermicompost and turf (1.0% m/v) dissolved in 0.02 mol L^{-1} NaHCO_3 were evaluated. To perform these studies, the μP_2 and μP_3 were activated with 9 and 15 pulses, respectively, to insert 51.8 $\mu\text{g L}^{-1}$ of Zn^{2+} and 47.7 $\mu\text{g L}^{-1}$ of Pb^{2+} ions solutions into the EFC. The μP_4 was used to add the solutions of the potential interferents into the EFC in concentrations ranging from 1:1, 1:10, and 1:100 (analyte: interferent) ratio.

Result and discussion

Pretreatment of the SPE-BDD

Before starting the electroanalytical chemistry procedures, appropriate pretreatments were performed on the BDD surface. For this, a cathodic pretreatment (CPT) and anodic pretreatment (APT) were applied by chronopotentiometry.

In studies described in the literature, current densities in the range from 500 to 1000 mA/cm^2 were employed.^{18,25} However, the CE based on graphite carbon embedded in the SPE-BDD cannot be used at such high current densities, because of its higher electrical resistance compared to the platinum electrodes that are generally used as CE. In fact, overloads of potentials were observed, since the generated potential exceeded the compliance of the commercial galvanostat used, *i.e.*, ± 12 V. To overcome this drawback, pretreatment with milder current densities was used: 25, 50, and 100 mA/cm^2 . In practical terms, a current of 12.85 mA was applied in the BDD (25.7 mm^2 geometric area) to achieve the 50 mA/cm^2 . The APT and CPT were applied for 60 s and 120 s respectively.

Fig. S2 shows the results obtained from the pretreatment on the BDD surface employing the chronopotentiometry in 0.1 mol L^{-1} H_2SO_4 solution, which was added by the μP_5 . The influence of the pretreatment was evaluated using a 1.0×10^{-3} mol L^{-1} solution of potassium hexacyanoferrate (III) in 0.1 mol L^{-1} KCl by cyclic voltammetry at a potential scan rate of 50 mV s^{-1} . For this, the μP_1 was activated and triggered with SV_1 applying 14 pulses to add this solution into the EFC. For this study, the temperature was thermostated at $25 \pm 1^\circ\text{C}$.

In Fig. S2 (A), the influence of the pretreatment in the electrochemical response of the BDD electrode can be clearly observed applying a current density of +50 mA/cm² during 60 s for APT and -50 mA/cm² during 120 s for CPT. Fig. S2 (B) presents a comparative result of the APT and CPT effect on the BDD electrode when applying these aforementioned current densities for 60 s. In Fig. S2 (C), the influence of the current density was evaluated for CPT during 120 s. The cyclic voltammograms for comparison between the performance of the pseudo-RE (Ag/AgCl) and the CE based on graphite carbon (CE-C) embedded into the SPE-BDD and the use of external CE and RE based on platinum foil (0.60 cm²) and an Ag/AgCl (3.0 mol L⁻¹ KCl), respectively, are presented in Fig. S2 (D).

According to the results shown in Fig. S2, the following considerations can be highlighted: i) Pretreatments of the SPE-BDD were needed; ii) There were no significant differences between the APT and CPT on the BDD surface; iii) The current densities of 25, 50, and 100 mA/cm² showed similar results, and 50 mA/cm² was chosen because it provided a good repeatability with low evolution of H_{2(g)} and O_{2(g)}; iv) The SPE-BDD presented current profiles similar to those obtained using an external counter and reference electrode, and only a shift in the potential was noted.

Supporting electrolyte study employing cyclic voltammetry

The phosphate, acetic acid/acetate, and BR buffer solutions and the sulfuric acid were evaluated to find the best supporting electrolyte for determination of Zn²⁺ and Pb²⁺ using cyclic voltammetry. The electrochemical parameters evaluated were the residual current, the potential window (mainly due to the over-potential for H_{2(g)} and O_{2(g)}), and the electrochemical profile. The acetic acid/acetate buffer solution, pH 4.0, and 0.1 mol L⁻¹ H₂SO₄ were the most suitable supporting electrolytes. However, the acetic acid/acetate buffer solution was chosen because the voltammograms presented a lower residual current and the widest potential window, Fig. S3.

Optimization of DPASV parameters

The DPASV optimization depends on the preconcentration step, mainly for the potential and time.¹⁴ Thus, for simultaneous determination of Zn²⁺ and Pb²⁺, the maximum current peaks (I_p) were obtained until -1.4 V, after which the current increased mainly due to the high H_{2(g)} evolution. Moreover, pulse amplitude (a) of 90 mV, pulse width (τ) of 5 ms, and sweep rate (v) of 50 mV s⁻¹ were the best parameters, generating a narrower width at half-height peak (ΔE_{p1/2}) with higher I_p. These parameters were applied using FBA approach.

Analytical curves obtained by employing FBA-DPASV

Aiming to construct analytical curves simultaneously for Zn²⁺ and Pb²⁺ ions, stock solutions of these ions were inserted into the EFC by switching ON the μP₂ and μP₃, as described in Fig. S1, employing the FBA system. Moreover, the acetic acid/acetate buffer solution at pH 4.0 was added by triggering μP₁ and SV₁. The analytical curves are presented in Fig. 4, and the main results are summarized in Table 1.

According to Table 1, a good analytical sensitivity and low limit of detections (LDs) were acquired, mainly for Pb²⁺ ions. In fact, LDs of 0.19 and 0.62 μg L⁻¹ (S/N = 3) and relative standard deviations (RSD) of 2.0% and 7.8% for 7.0 μg L⁻¹ Pb²⁺ and 34.5 μg L⁻¹ Zn²⁺, respectively, were attained at a sampling frequency of 12 h⁻¹. These good analytical performances demonstrate the applicability and repeatability of the developed method.

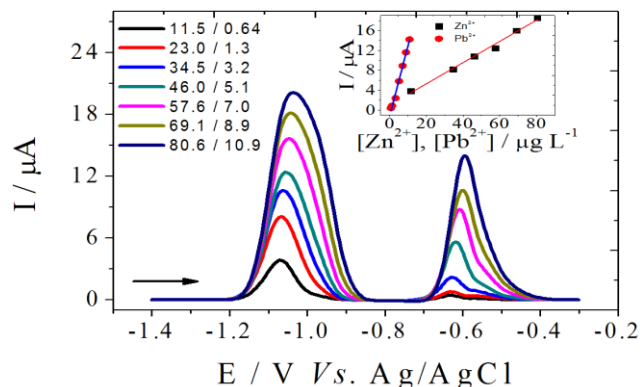


Fig. 4. Simultaneous analytical curves for Zn²⁺ and Pb²⁺ using FBA-DPASV. Parameters for the DPASV: a = 90 mV, τ = 5 ms, and v = 50 mV s⁻¹ with potential and preconcentration time of -1.4 V and 180 s, respectively.

Table 1. Analytical parameters obtained applying FBA-DPASV approach.

Analytical performance parameters	Zn ²⁺	Pb ²⁺
Sensitivity / (μA / μg L ⁻¹)	0.21	1.41
Coefficient of regression (r)	0.990	0.991
Limit of detection / μg L ⁻¹	0.62	0.19
Limit of quantification / μg L ⁻¹	2.10	0.62
Linear range / μg L ⁻¹	11.5 – 80.6	0.64 – 10.9
Repeatability (RSD) ^a	7.8 % / 34.5	2.0 % / 7.0

^aRSD with n = 3 per analyte concentration in μg L⁻¹.

Interference study employing FBA-DPASV

The following ions were evaluated in the interference studies: Li⁺, K⁺, Na⁺, Mg²⁺, Ca²⁺, Fe³⁺, Cl⁻, CO₃²⁻, SO₄²⁻, PO₄³⁻, NO₃⁻, Ni²⁺, Cu²⁺, Al³⁺, Hg²⁺, Cr³⁺, and Mn⁵⁺, as well as humic acid. From all ions evaluated, only Cu²⁺ and Hg²⁺ at a 1:1 ratio (47.7 and 51.8 μg L⁻¹, respectively) presented a 10% interference during determination of Zn²⁺ and Pb²⁺ ions. For humic acid, an interference of 10% was found at a concentration of 0.01% (m/v). No significant interference was found for other ions at the studied concentration levels.

Recovery and accuracy studies using FBA-DPASV

The recovery study was carried out with water samples acquired from the pretreatment of water substations (SANEPAR, Brazil) (A), wastewater from the petrochemical industry (Petrobras, Brazil) (B), seawater (Alicante-Spain) (C), and wastewater from the Department of Chemistry (DQ) from the University of São Carlos (São Carlos, Brazil) (D). Additions of three different concentrations in triplicate were performed using the FBA system. For this, aliquots of standard solutions of the analytes were added to the samples in the EFC by employing μP₂ and μP₃, respectively. In these studies, only 100 μL of the samples were inserted into EFC applying 5 pulses to μP₆. For the samples A and B, the recovery studies were carried out by adding Pb²⁺ and Zn²⁺ ions, in sample C only Pb²⁺, and in sample D only Zn²⁺ were analyzed as described in Table 2.

Table 2. Recovery test using the FBA-DPASV approach.

Sample	Added / $\mu\text{g L}^{-1}$		Found / $\mu\text{g L}^{-1}$		Recovery / (%)	
	Pb ²⁺	Zn ²⁺	Pb ²⁺	Zn ²⁺	Pb ²⁺	Zn ²⁺
	1.9	23.2	1.7±0.1	23.5±0.4	89.5	101
A	3.8	57.6	3.9±0.1	57.0±0.8	103	99.0
	5.7	80.6	5.9±0.1	84.6±0.7	104	105
	0.6	11.5	0.6 ±0.1	10.9±0.2	100	94.8
B	2.5	23.0	2.6±0.1	24.5±0.3	104	107
	6.4	46.0	5.8±0.2	44.8±0.9	89.7	97.4
C	1.3	-	1.2±0.5	-	92.3	-
	5.1	-	5.3±0.3	-	104	-
	10.9	-	11.3±0.3	-	104	-
	-	23.0	-	24.2±0.5	-	105
D	-	46.0	-	48.6±0.9	-	106
	-	69.1	-	66.6±0.5	-	96.4

According to the results shown in Table 2, the recovery tests were very acceptable, and ranged from 89.5% to 107%, suggesting that potential interfering compounds were not present or that they were not found at concentrations above those evaluated in the interference studies.

The accuracy of the method was checked by measurement of certified river water (1643e Trace Elements in Water, NIST) with concentrations of Zn²⁺ and Pb²⁺ of $78.5 \pm 2.2 \mu\text{g L}^{-1}$ and $19.63 \pm 0.21 \mu\text{g L}^{-1}$, respectively. After performing the standard addition method with $n = 5$, the concentrations supplied by the FBA-DPASV were: $79.5 \pm 0.6 \mu\text{g L}^{-1}$ and $19.2 \pm 0.4 \mu\text{g L}^{-1}$, respectively. The estimated t -unpaired values found were 2.36 and 1.52, which are in very close agreement at a confidence level of 95%, t -test (4, 95%) = 2.78.

According to the analytical data obtained, the electrochemical method based on FBA-DPASV provides good precision and accuracy to determine Pb²⁺ and Zn²⁺ ions in water samples individually or simultaneously. Furthermore, a low consumption of reagents with low waste generation of only 700 μL , and a sampling frequency of 12 h^{-1} were acquired.

Optimization of the MPA method

The present data were obtained by measuring the transient signals using MPA detection applying the MCFA system. As described, the μP_1 was continuously triggered simultaneously with SV_1 to pump the supporting electrolyte solution at a constant flow rate of $50 \mu\text{L s}^{-1}$. The other μP_s were used for the injection of standard solutions of Zn²⁺ and Pb²⁺ ions for single or simultaneous determinations, according to the experimental procedures described in the Fig. S1.

As the technique of multiple pulse amperometry consists essentially of applying potential pulses sequentially in a relatively short time,^{21,23,25} two main parameters were optimized: 1) applied potential pulses, and 2) time duration of each pulse. The pulses were applied in a range from -0.4 to -1.5 V, constructing hydrodynamic voltammograms as presented in Fig. S4. Moreover, the potential pulses were evaluated in the time ranging from 50 to 500 ms, as shown in Fig. S5.

As can be seen for the single determination of Zn²⁺ and Pb²⁺, the most appropriate potentials were -1.5 V and -1.3 V, respectively. However, as the main purpose of the application of MPA consists of simultaneous determinations, the compromise between higher peak current and selectivity was studied. Thus, the best potential applied for the determination of Pb²⁺ was -1.0 V, in which negligible reductions of Zn²⁺ were obtained. For Zn²⁺ ions, the appropriate potential was -1.4 V. Furthermore, these potentials were chosen because of the low and stable baseline current, to avoid possible interference when analyzing complex matrices, and the evolution of H_{2(g)}, which harms the repeatability. Moreover, for single electrochemical analyses, -0.9 V and -1.3 V can also be used for Pb²⁺ and Zn²⁺ determinations.

In Fig. S5, the results for hydrodynamic studies regarding time of the potential pulses are presented. A decrease in the time of the potential applied produced a large reduction in the peak current in all cases. Indeed, pulses applied for short times generated fast reduction during the passage of the sampling zone by the SPE-BDD, and thus, 50 ms or 100 ms is preferable. Because of this, for simultaneous measurements, -1.0 V for 50 ms was applied for Pb²⁺ determination in which the oxidation of Zn forming Zn²⁺ ions was avoided. For less negative potentials, e.g., -0.9 V, a long time, such as 600 ms, should be used to determine Pb²⁺ without harming the Zn²⁺ determination.

Optimization of the MCFA system employing MPA

The parameters evaluated for the MCFA system were the flow rate of the carrier solution and the size of the sampling volume. For this, the flow rate ranged from 1.0 to 9.0 mL min^{-1} (16 to 150 $\mu\text{L s}^{-1}$) employing the μP_1 with pulse frequencies from 1 to 12 Hz with the SV_1 switched ON, and simultaneous actuation of μP_3 for addition of the Pb²⁺ solutions was performed. The results are presented in Fig. S6. Only the data relating to the Pb²⁺ ions are presented, since a similar behavior was observed for Zn²⁺ ions. As can be noted, for higher flow rates, an increase in the current was observed, since the mass transport towards the surface of SPE-BDD increased, due to a thinner diffusion layer that was reached. Thus, a limited flow rate was obtained at 125 $\mu\text{L s}^{-1}$, where the reduction current was almost constant.²³ However, a lower and more stable baseline current was obtained at a flow rate of 50 $\mu\text{L s}^{-1}$. Thus, for a better compromise between the analytical signal and the sampling frequency, a flow rate of 50 $\mu\text{L s}^{-1}$ was selected for further electrochemical experiments.

For studies of the sample volume injected into the EFC, sampling pulses or sampling cycles from 1 to 35 equal to 20–700 μL were performed using μP_2 or μP_3 (20 μL per pulse) for insertion of Zn²⁺ and Pb²⁺ ions solutions into the EFC as shown in Fig. S7.

The volume of sampling is equivalent to the volume of the looping of sampling employed in the traditional FIA approach, since the number of pulses for each μP is proportional to the injected volume into the EFC.^{24–26} As shown in Fig. S7, a linear correlation was observed between the sampled current and the number of pulses in the range from 1 to 15 (20 to 300 μL) for Zn²⁺ solution and from 1 to 25 (20 to 500 μL) for Pb²⁺ ions solution. For aliquots greater than 300 μL and 500 μL for Zn²⁺ and Pb²⁺, respectively, the current was kept almost unchanged.

Application of the MPA for simultaneous determination

For simultaneous determination, the best potential and time applied were evaluated (Fig. 5). For this study, the stock solution of Zn²⁺ and Pb²⁺ ions were added into the EFC by μP_2 ,

and μP_3 , respectively, triggering μP_1 with the SV_1 switched ON, according to that described in Fig. S1. After this, simultaneous measurements were performed employing the MPA for $-0.9\text{ V}/600\text{ ms}$, $-1.0\text{ V}/50\text{ ms}$, $-1.2\text{ V}/50\text{ ms}$, and $-1.4\text{ V}/50\text{ ms}$, as presented in Fig. 5.

Firstly, just the μP_2 was switched ON to add $100\text{ }\mu\text{L}$ of a Zn^{2+} ions stock solution ($10,000\text{ }\mu\text{g L}^{-1}$) into the EFC in triplicate, aiming to evaluate the amperograms for single determination in each applied potential. For the same purpose, the μP_3 was switched ON to inject $160\text{ }\mu\text{L}$ of a Pb^{2+} ions stock solution ($2000\text{ }\mu\text{g L}^{-1}$) in triplicate. After this, simultaneous additions were performed to inject $180\text{ }\mu\text{L}$ of Pb^{2+} and $300\text{ }\mu\text{L}$ of Zn^{2+} solutions ($n = 3$). Further, the single determinations were again carried out with $300\text{ }\mu\text{L}$ of Zn^{2+} ($n = 2$) and $200\text{ }\mu\text{L}$ of Pb^{2+} ($n = 2$) to evaluate the possible effect of memory and the repeatability of the results by MCFA-MPA.

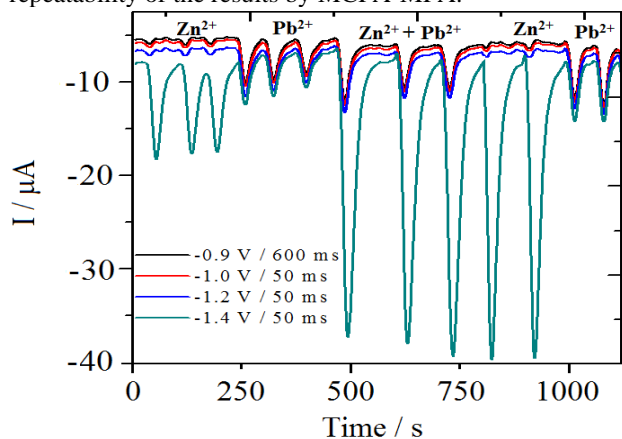


Fig. 5. Amperograms of the simultaneous determination of Zn^{2+} and Pb^{2+} ions using SPE-BDD with MCFA-MPA applying four pulses of potential: $-0.9\text{ V}/600\text{ ms}$, $-1.0\text{ V}/50\text{ ms}$, $-1.2\text{ V}/50\text{ ms}$, and $-1.4\text{ V}/50\text{ ms}$. Carrier solution: acetic acid/acetate buffer, pH 4.0 at a flow rate of $32\text{ }\mu\text{L s}^{-1}$. Stock solutions: $10,000\text{ }\mu\text{g L}^{-1}$ and $2000\text{ }\mu\text{g L}^{-1}$ for Zn^{2+} and Pb^{2+} ions, respectively.

As can be seen in Fig. 5, most of the Pb^{2+} ions were reduced applying a pulse of -0.9 V for 600 ms . Pulse times smaller than this, which increased the current obtained, yielded a decrease in the Zn^{2+} current, because at this potential Zn was oxidized. Thus, $-0.9\text{ V}/600\text{ ms}$, $-1.0\text{ V}/50\text{ ms}$, or $-1.2\text{ V}/50\text{ ms}$ could be applied. However, $-1.0\text{ V}/50\text{ ms}$ was chosen since a stable and a low baseline current to detect the Pb^{2+} ions was obtained with a negligible Zn^{2+} reduction. At the potential of -1.4 V , both ions were reduced. At this potential, the signal of the current obtained correlated with the concentration of the Zn^{2+} ions, which was calculated by simple subtraction of the current obtained during determination of Pb^{2+} ions. It was possible since the current measured for Pb^{2+} ions at -1.4 V was similar to that acquired at -1.0 V .

Moreover, the very stable baseline currents and the narrow amperograms show the applicability of the EFC developed for measurement of transient signals, as for MPA. According to this procedure, the analytical curves for the Zn^{2+} and Pb^{2+} simultaneous determination were successfully carried out.

Application of MCFA-MPA and comparative method

In order to demonstrating the performance of the MCFA system and the MPA for metal ion detection, analytical curves and further analysis of the samples were performed for simultaneous determination of Zn^{2+} and Pb^{2+} ions (Fig. S8). However, previously, the samples were spiked with stock

solutions of Zn^{2+} and Pb^{2+} ions in order to be measured by the MCFA-MPA and the comparative method.

For analyses of these ions, the μP_1 was continuously switched ON with simultaneous activation of SV_1 , μP_2 , and μP_3 as shown in Fig. S1. The samples analyzed were as follows: water samples obtained from the pretreatment of water substations (SANEPAR) (A1 and A2), samples collected from the Monjolino Lake in São Carlos (A3 and A4), and wastewater and tap water from the Department of Chemistry from the Federal University of São Carlos (A5 and A6).

Table 3 presents the best analytical parameters obtained for simultaneous determination of Zn^{2+} and Pb^{2+} ions.

Table 3. Analytical performance acquired using MCFA-MPA.

Analytical parameters	Zn^{2+}	Pb^{2+}
Sensitivity / ($\mu\text{A} / \mu\text{g L}^{-1}$)	0.0063	0.0195
Coefficient of regression (r)	0.994	0.990
Limit of detection / $\mu\text{g L}^{-1}$	220.0	41.0
Limit of quantification / $\mu\text{g L}^{-1}$	730	140
Linear range / $\mu\text{g L}^{-1}$	830 – 4980	140 – 820
Repeatability (RSD) ^a	2.3%/ 1990	1.5%/ 330

^aBased on RSD, $n = 3$ per analyte concentration in $\mu\text{g L}^{-1}$.

Table 4 presents the results for the determination of the spiked samples employing the method based on MCFA-MPA.

Table 4. Determination Zn^{2+} and Pb^{2+} in spiked samples.

	Spiked concentration /		MCFA-MPA / $\mu\text{g L}^{-1}$		Relative error / %	
	Pb^{2+}	Zn^{2+}	Pb^{2+}	Zn^{2+}	Pb^{2+}	Zn^{2+}
A1	650	2000	627 ± 1	1990 ± 1	-3.5	-0.5
A2	650	2000	626 ± 1	1924 ± 1	-3.7	-3.8
A3	350	1500	355 ± 1	1436 ± 1	1.4	-4.3
A4	350	1500	345 ± 1	1600 ± 1	-1.4	6.7
A5	450	3500	441 ± 1	3398 ± 1	-2.0	-2.9
A6	800	4500	850 ± 1	4599 ± 1	6.3	2.2

The simultaneous determination of Zn^{2+} and Pb^{2+} ions with the developed method supplied detection limits of 220.0 and $41.0\text{ }\mu\text{g L}^{-1}$, respectively, with a sampling frequency of 67 h^{-1} and with only $700\text{ }\mu\text{L}$ of residue generated per determination.

With the obtained results, it is possible to evaluate the good performance of the method developed. In fact, low standard deviations and relative errors smaller than 7.0% were acquired. These good results are based on selectivity appreciable of the MPA using the SPE-BDD, where the time to deposition is reduced, and the adsorption of metal ions on the electrode surface is minimum leading to a negligible interference.

To certify the accuracy of the MCFA-MPA approach, the ICP-OES method was employed as a comparative method. By comparison, the data acquired for both methods employing the

spiked samples, the *t*-paired values were 0.25 and 0.48 for Zn²⁺ and Pb²⁺, respectively, which is in very close agreement at a confidence level of 95%, *t*-test (2, 95%) = 4.30.

The versatility of the EFC developed was remarkable, in which two distinct electrochemical flow methods were performed without any physical changes, *i.e.*, MCFA-MPA and FBA-DPASV approaches. Furthermore, other electrochemical methods, *e.g.*, cyclic voltammetry and chronopotentiometry were applied. In addition, using the EFC, there is no need for sample handling, nor the preparation of various standard solutions to construct the analytical curve, since solutions of different concentrations were on-line prepared from a single stock solution under a thermostated control of 25 ± 1°C.

Conclusions

The high versatility of the EFC allows to carry out both FBA-DPASV and MCFA-MPA approaches with good repeatability, accuracy and sensitivity. The method using MCFA-MPA for the simultaneous determination of Pb²⁺ and Zn²⁺ supplied LDs of 41.0 and 220.0 µg L⁻¹, respectively, which, when compared to those obtained using FBA-DPASV (0.19 µg L⁻¹ and 0.62 µg L⁻¹ for Pb²⁺ and Zn²⁺) were 200 and 300 times higher, respectively. On the other hand, if the sampling frequency is a paramount factor, *e.g.*, for routine analyses, the method by MCFA-MPA was *ca.* 6 times more efficient. The temperature control, versatility, robustness, and low waste generation (700 µL) were the main features of the developed electrochemical methods making them very useful for environmental applications. Moreover, these methods are in close agreement with the green chemistry approach and sustainable research.

Acknowledgements

The authors acknowledge the CAPES, CNPq, and FAPESP (Proc. N° 2010/11690-0, 2011/23598-3 and 2013/ 14993-1) for the financial support and scholarships supplied.

Notes and references

^a Departamento de Química, Universidade Federal de São Carlos, Centro de Ciências Exatas e de Tecnologia, 676, 13565-905, São Carlos, São Paulo, Brazil. Email: vagnerlaqa@gmail.com. Phone: +55 11 30913781.

^b Empresa Brasileira de Pesquisa Agropecuária, Embrapa Solos, Rio de Janeiro, RJ - Brazil.

Electronic Supplementary Information (ESI) available: See DOI: 10.1039/b000000x/

- [1] A. Kraft, *Int. J. Electrochem. Sci.*, 2007, **2**, 355-385.
- [2] S. E. W. Jones and R. G. Compton, *Curr. Anal. Chem.*, 2008, **4**, 170-176.
- [3] Y. Zhou and J. Zhi, *Talanta*, 2009, **79**, 1189-1196.
- [4] S. Szunerits and R. Boukherroub, *J. Solid State Electrochem.*, 2008, **12**, 1205-1218.
- [5] L. S. Andrade, M. C. de Moraes, R. C. Rocha-Filho, O. Fatibello-Filho and Q. B. Cass, *Anal. Chim. Acta*, 2009, **654**, 127-132.
- [6] R. A. Medeiros, A. E. de Carvalho, R. C. Rocha-Filho and O. Fatibello-Filho, *Talanta*, 2008, **76**, 685-689.
- [7] C. A. Martinez-Huitle and E. Brillas, *Appl. Catal. B: Environ.*, 2009, **87**, 105-145.

- [8] G. F. Pereira, L. S. Andrade, R. C. Rocha-Filho, N. Bocchi and S. R. Biaggio, *Electrochim. Acta*, 2012, **82**, 3-8.
- [9] G. F. Pereira, R. C. Rocha-Filho, N. Bocchi and S. R. Biaggio, *Chem. Eng. J.*, 2012, **198**, 282-288.
- [10] M. Panizza and G. Cerisola, *Electrochim. Acta*, 2005, **51**, 191-199.
- [11] T. Kondo, H. Sakamoto, T. Kato, M. Horitani, I. Shitanda, M. Itagaki and M. Yuasa, *Electrochem. Commun.*, 2011, **13**, 1546-1549.
- [12] G. R. S. Banda, Y. Einaga and C. A. Martinez-Huitle, Hindawi Publishing Corporation, 2012, DOI: 10.1155/2012/548504.
- [13] P. Sonthalia, E. McGaw, Y. Show and G. M. Swain, *Anal. Chim. Acta*, 2004, **522**, 35-44.
- [14] A. Manivannan, R. Kawasaki, D. A. Tryk and A. Fujishima, *Electrochim. Acta*, 2004, **49**, 3313-3318.
- [15] C. Prado, S. J. Wilkins, P. Grundler, F. Marken and R. G. Compton, *Electroanal.*, 2003, **15**, 1011-1016.
- [16] O. El Tall, N. Jaffrezic-Renault, M. Sigaud and O. Vittori, *Electroanal.*, 2007, **19**, 1152-1159.
- [17] E. A. McGaw and G. M. Swain, *Anal. Chim. Acta*, 2006, **575**, 180-189.
- [18] L. S. Andrade, R. C. Rocha-Filho, Q. B. Cass and O. Fatibello-Filho, *Anal. Methods*, 2010, **2**, 402-407.
- [19] E. M. Richter, D. P. de Jesus, C. A. Neves, C. L. do Lago and L. Angnes, *Quim. Nova*, 2003, **26**, 839-843.
- [20] M. E. Snowden, P. H. King, J. A. Covington, J. V. Macpherson and P. R. Unwin, *Anal. Chem.*, 2010, **82**, 3124-3131.
- [21] F. S. Felix and L. Angnes, *J. Pharm. Sci.*, 2010, **99**, 4784-4804.
- [22] D. T. Gimenes, P. F. Pereira, R. R. Cunha, R. A. B. da Silva, R. A. A. Munoz and E. M. Richter, *Electroanal.*, 2012, **24**, 1805-1810.
- [23] W. T. P. dos Santos, D. T. Gimenes, E. M. Richter and L. Angnes, *Quim. Nova*, 2011, **34**, 1753-1761.
- [24] A. C. V. Lopes, R. D. S. Luz, F. S. Damos, A. S. dos Santos, D. L. Franco and W. T. P. dos Santos, *J. Braz. Chem. Soc.*, 2012, **23**, 1800-1806.
- [25] R. A. Medeiros, B. C. Lourencao, R. C. Rocha-Filho and O. Fatibello-Filho, *Anal. Chem.*, 2010, **82**, 8658-8663.
- [26] V. B. dos Santos, E. L. Fava, N. S. M. Curi, R. C. Faria and O. Fatibello-Filho, *Talanta*, 2014, **126**, 82-90.
- [27] B. F. Reis, M. F. Gine, E. A. G. Zagatto, J. L. F. C. Lima and R. A. Lapa, *Anal. Chim. Acta*, 1994, **293**, 129-138.
- [28] L. F. Almeida, M. G. R. Vale, M. B. Dessuy, M. M. Silva, R. S. Lima, V. B. dos Santos, P. H. D. G. Diniz and M. C. U. de Araujo, *Talanta*, 2007, **73**, 906-912.
- [29] L. C. S. de Figueiredo-Filho, B. C. Janegitz, O. Fatibello-Filho, L. H. Marcolino-Junior and C. E. Banks, *Anal. Methods*, 2013, **5**, 202-207.
- [30] L. C. S. de Figueiredo-Filho, V. B. dos Santos, B. C. Janegitz, T. B. Guerreiro, O. Fatibello-Filho, R. C. Faria and L. H. Marcolino-Junior, *Electroanal.*, 2010, **22**, 1260-1266.
- [31] D.-Q. Huang, B.-L. Xu, J. Tang, L.-L. Yang, Z.-B. Yang and S.-P. Bi, *Int. J. Electrochem. Sci.*, 2012, **7**, 2860-2873.